Title: In Situ Formation of Metal Carbide Catalysts

Authors: Megan M Moyer; Canan Karakaya; Robert J. Kee; Brian Trewyn, Ph.D

To be cited as: 10.1002/cctc.201700304

Link to VoR: https://doi.org/10.1002/cctc.201700304

In Situ Formation of Metal Carbide Catalysts

Megan M. Moyer,[a] Canan Karakaya,[b] Robert J. Kee, [b] Brian G. Trewyn[a]*

Abstract: Metal carbide catalysts are essential to many widely used chemical processes. Fischer-Tropsch synthesis, methane dehydroaromatization, and biomass conversion catalysts are typically prepared *in situ* from a metal oxide precursor with a carbon-containing gas. The reduction process of the metal oxide affects the final catalyst, as does the carburization gas mixture, and metal promoters. By looking at materials that are carburized *in situ,* new insights can be gained about catalyst activation, fuel processing, and deactivation stages. The main focuses of this review are iron carbide, molybdenum carbide, and nickel carbide; analyzing catalyst synthesis methods, reduction steps, *in situ* carburization, and improvements to the native processes. By combining years of research on these catalysts, trends and similarities are observed that can be used to improve current catalytic studies.

1. Introduction

One of the fundamental pillars of green chemistry is the utilization of catalysts to eliminate hazardous wastes and undesirable side-products. Using catalysis, many traditional chemical processes can be improved to be more efficient.[1] An alternative fuel process that utilizes these principles is Fischer-Tropsch synthesis (FTS). This chemical pathway has been used for over 90 years to transform natural gas, coal, and biomass precursors into useful hydrocarbon products over catalysts such as iron carbide and Ni^0 metal.[2] The fuels produced from this process are more environmentally friendly than those produced through conventional petroleum pathways.[3] The world's current fuel and chemical production relies heavily on petroleum crude oil, though reserves of methane and coal exceed that of crude oil by factors of 1.5 and 25, respectively.[4] Geological methane contributes 16-40 terragrams of natural gas to the atmosphere annually; therefore the ability to use this as a source for energy is highly desired.[5, 6] With climate change as one of the most prevalent concerns today, finding green pathways to converting this gas into useful hydrocarbon products is the focus of both academic and industrial scale research.[7] One such process that has emerged for the direct conversion of methane to higher hydrocarbons is methane dehydroaromatization (MDA). This catalytic process employs a bifunctional catalyst consisting of low cost molybdenum catalysts on zeolite to form higher value products like benzene and hydrogen gas.[8] Another key aspect to improve fossil fuel consumption is creating more direct chemical pathways that minimize the production of carbon dioxide. By either incorporating this gas into chemical pathways that produce useful hydrocarbons or finding alternative pathways that are CO_2 free, improvements to the atmosphere and reductions in energy consumption can be made. Biomass conversion can be used in the production of essential chemicals including liquid transportation fuels to reduce the amount of CO_2 in the atmosphere and create a more sustainable energy source than petroleum.[9, 10] Common to all of these catalytic processes are metal carbide

[a] Mrs. M. M. Moyer, Prof. B. G. Trewyn
Department of Chemistry
Colorado School of Mines
1500 Illiniois St. Golden, CO 80401
E-mail: btrewyn@mines.edu
[b] Prof. C. Karakaya, Prof. R. J. Kee
Mechanical Engineering
Colorado School of Mines
1500 Illinois St. Golden, CO 80401

catalysts that are formed during the reaction, an *in situ* process. To to best of our knowledge, there is no comprehensive review that compiles information on *in situ* formed metal carbide catalysts across multiple applications. This review will discuss the types of chemistry where these catalysts are applied, the precursor materials, current understanding of the carburization mechanisms for the catalysts, and improvements to the catalytic materials.

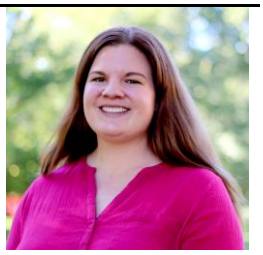

Megan Moyer received her B.Sc. in Chemistry with a specialty in Biochemistry from Colorado School of Mines in 2013. She joined Prof. Trewyn's research group in 2013 and is currently a PhD candidate in the Applied Chemistry program. Her research focus includes work on microporous and mesoporous support materials for catalysis in applications such as gas to liquid, catalytic cracking, and tandem catalysis.

Prof. Canan Karakaya received her Ph.D from Karlsruhe Institute of Technology, Germany in December, 2012. She joined the Colorado School of Mines in February 2013 as a postdoctoral fellow. She currently holds a Research Asst. Professorship in CSM, Mechanical Engineering Department and working on various chemical processes including oxidative coupling of methane, SiC epi-growth, gas-to-liquid catalysis and H_2 generation from reforming of ethanol.

Prof. Robert Kee holds the George R. Brown Distinguished chair. Dr. Kee's research interests are primarily in modeling and simulation of chemically reacting fluid flow. Applications are generally in the area of clean energy, including fuel cells, photovoltaics, and advanced combustion. Recent research includes efforts on catalytic-combustion and water-mist flame suppression.

Prof. Brian G. Trewyn received his Ph.D. from Iowa State University (ISU) in 2006. After working as the associate director of the Center for Catalysis and adjunct professor at ISU, he joined the faculty at Colorado School of Mines (CSM) in 2012. He is currently an Assistant Professor of Chemistry and a faculty member of the Material Science Program at CSM. His research focuses on biological and catalytic applications for high surface area, porous materials.

2. Chemical Processes

2.1. Fischer-Tropsch Synthesis Chemistry

One of the most common reactions that typically requires a carburized catalyst is Fischer-Tropsch synthesis (FTS), which converts syngas (CO and H_2) into hydrocarbon products. Fischer-Tropsch chemistry has been studied for many years, with the first report nearly a century ago[11-13] and is an industrialized process for gas to liquid conversion. The reaction requires a metal catalyst with the most common metals being iron and cobalt.[14] This reaction is important as an alternative to oil as a feedstock, but the products of FTS must be further upgraded in order to be utilized as fuel in the current infrastructure. Reaction temperatures are generally in the range of 473-613 K, with some low temperature processes run around 423 K.[15] Reaction pressures are approximately 1-10 atm, though lower pressure syntheses cause less strain on most equipment. Syngas conversion to hydrocarbons via FTS is simply written as a balanced equation (Eq. 1):

$$nCO + (2n+1)H_2 \rightarrow C_nH_{2n+2} + nH_2O \quad \text{Eq. 1}$$

There are, however, numerous side reactions that compete with the formation of hydrocarbon products. A reaction that frequently occurs with iron-based catalysts is a water-gas shift (WGS).[16] In this reaction, carbon monoxide and water react to form molecular hydrogen and carbon dioxide

$$CO + H_2O \rightleftarrows H_2 + CO_2 \quad \text{Eq. 2}$$

leading to the formation of longer hydrocarbon chains during FTS even if hydrogen is not an abundant reactant. Another unique feature of FTS is that it can be employed with a multitude of reactants including coal, natural gas, and biomass. In this respect, it is one of the most useful and versatile chemical pathways to produce cleaner energy. The hydrocarbons produced from this process are environmentally-friendly as they are free from sulfur, nitrogen, and

aromatic hydrocarbons, making the subsequent fuels produced from FTS also cleaner than conventional petroleum-based fuels.[17] Despite over 90 years of progress and research in this field, there are still many challenges to FTS including limiting undesirable side reactions and increasing the amount of desirable products that can be easily upgraded to usable fuels. Many reports focus on improving the catalyst as it directly affects the types of products, amount of products, reaction pathways, and side reactions like WGS.

Two of the most productive metals employed as FTS catalysts are iron and cobalt, both for their high catalytic activity as well as their relative low costs and earth abundance, allowing for industrial scale production. The activity of the iron catalyst is initially low until carbide species are formed whereas cobalt metal tends to be active from the onset of the reaction.[18] Iron carbide is generally formed *in situ* under the presence of CO and H_2 gas (Scheme 1). The carburization of the iron metal allows for CH_x species to form on the surface of the catalyst that then undergo polymerization to form high hydrocarbon intermediates and final products.[17]

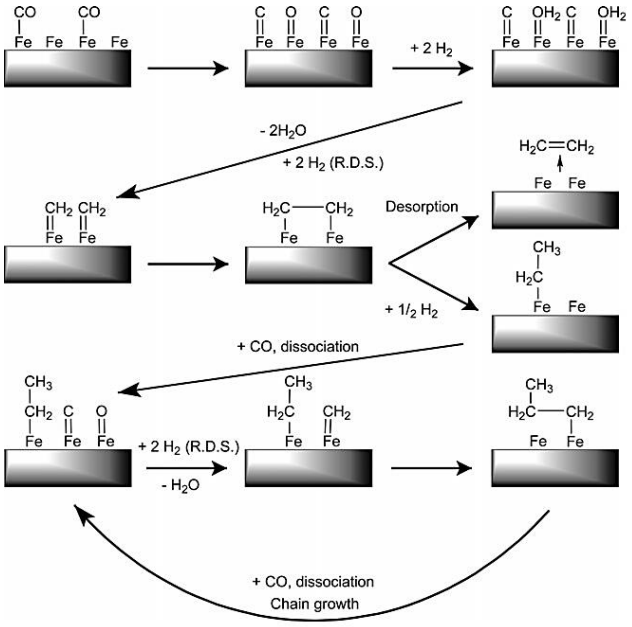

Scheme 1. Possible reaction mechanism for *in situ* carburization of the catalyst surface during Fischer Tropsch Synthesis. Reduction of surface iron oxide is followed by carburization of the metal.[14]

Since the iron carbide is able to catalyze WGS, a wide range of chemical products is possible using this approach. However, iron catalysts also undergo rapid deactivation, which requires expensive and time-consuming catalyst regeneration or replacement.[14] Research is heavily focused on understanding and preventing this deactivation and improving overall catalyst lifetime. In order to accomplish this, an in-depth understanding of the deactivation mechanism is required. Despite many years of research, this mechanism is not fully understood and even the nature and structure of the active catalyst remain a topic of debate. Different types of iron such as metallic iron, iron carbide, and iron oxide may be responsible for catalysis, or it may be a combination of different active species working synergistically, though it is generally agreed that iron carbide species are the active catalyst. Franz Fischer originally proposed that CO dissociation over the iron catalyst was the primary step in the reaction,

forming catalytic iron carbide. The carbon could then be hydrogenated to methylene species and polymerized to products.[11-13, 15] Generally a CH_x species is formed at the catalyst surface, but the exact monomer is not yet agreed upon.

Many of the challenges of understanding the iron-based catalysts apply also to cobalt catalysts, except Co does not form a carbide during the reaction. In some cases, the addition of cobalt assists the iron catalyst by tuning the active environment.[17] Ernst *et al*. and Bezemer *et al*. found that Co undergoes a similar reduction profile to iron when subjected to CO/H_2 gas. The oxide is first reduced from Co_3O_4 to CoO and finally to Co metal. However, instead of carburizing during the reaction, the active species has always been observed as metallic Co.[19, 20] Despite the challenges and uncertainties involved in the chemistry of FTS, there is a wide variety of research on the catalysts that provides insight into the importance of carbide catalysts formed with *in situ* carburization.

2.2. Methane Dehydroaromatization Chemistry

Methane dehydroaromatization (MDA) is a gas-to-liquid process that is conceivably a more direct route to producing liquid fuels than FTS chemistry. Methane is directly converted into benzene, hydrogen and traces of other hydrocarbon products over a bi-functional metal/zeolite catalyst, avoiding oxygenated intermediates; it is therefore often presented as a direct process to produce high energy density materials.[3, 21] However, methane is thermodynamically stable to high temperatures (above 973 K) and requires catalytic upgrading to form liquid molecules.[22, 23] The main products of MDA are benzene and hydrogen; napthalene is an undesired side product and ethylene and ethane can be formed at very low levels. Typical reaction conditions are 1 bar, 948-1073 K, and 750-4500 WHSV (ml $g_{catalyst}^{-1}$ h^{-1}).[24] The general reaction pathway for MDA is as follows:

$$6CH_4 \rightleftharpoons 9H_2 + C_6H_6 \qquad \text{Eq. 3}$$

this is idealized; the actual reaction is typically more complex. Essential to this process is the bi-functional catalyst. The methane is first activated on the metal catalyst (typically molybdenum) to form primarily ethylene and hydrogen, then further polymerization and aromatization reactions take place on the Brønsted acid sites of the zeolite.[25-27] The overall activity of the catalyst is not very high and even the best catalysts can only convert up to about 12% of the methane feed at 973-993 K.[28, 29] Additionally, the selectivity of the catalyst towards its desired product (benzene) is only about 60-80% with the other 20+% consisting largely of polyaromatic hydrocarbons that contribute to the rapid coking observed in these reactions.[6] The formation of coke, carbonaceous residues that block access to the catalyst active sites, during the MDA reaction deactivates the catalyst and causes the benzene formation rate to drop gradually over timetime at elevated temperature and pressure.[30]

Extensive research has been conducted on metal types, metal loadings, zeolite types, and zeolite structures in order to improve the efficiency of the MDA reaction. This process has not yet been commercialized due to thermodynamic limitations affecting methane conversion and benzene selectivity as well as rapid catalyst deactivation (within a few hours). As a result, much of the research in this area has been focused on the catalyst and finding ways to limit coke formation while increasing benzene selectivity. Attempts have been made to improve methane conversion by incorporating membranes that remove hydrogen as it is being produced, but these reactions still suffer from high naphthalene formation rates and coking.[31] Many different transition metals have been studied for MDA

including W, Re, Ga, and Co, however; the best performing metal is Mo, and it is most commonly studied for this chemistry.[6] The conversion of methane to hydrocarbon products is largely affected by the metal loading. It has been reported that conversion increases with increasing Mo loading up to 6 wt% Mo supported on zeolite. If Mo loading is further increased, activity begins to decrease as zeolytic acid sites are deactivated; many studies are performed with 2, 4, or 6 wt% Mo as these tend to work most efficiently.[32] Finally, the type of zeolite used alongside the metal catalyst plays an important role in MDA. Commonly used supports are ZSM-5 and H-MCM-22 type zeolites. ZSM-5 is often the choice of support for MDA due to its commercial availability as well as tunable acidity and favorable pore structure.[33] The unit cell of synthesized ZSM-5 is a = 20.07, b = 19.92, and c = 13.42 Å. The three dimensional channels in the zeolite are made of 10-membered rings (Figure 1) and it has a specific surface area of 300-350 m^2/g.[33, 34]

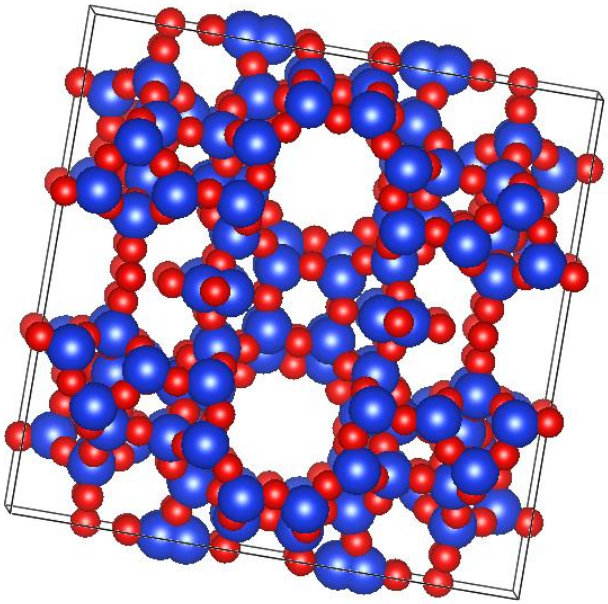

Figure 1. ZSM-5 framework viewed along the [010] access showing the 10-member ring pores.[34]

MCM-22 contains a two pore system consisting of a 10-member ring and a larger 12-member ring (Figure 2). The unit cell parameters are a = 14.11 and c = 24.88 Å.[35] During the synthesis, Al is partially extracted from the framework, leaving hydroxyl groups which act as very strong acid sites.[36] Typical surface areas are 400-500 m^2/g.[37]

MCM-22 is not commercially available, making ZSM-5 the more investigated support. More recently, nanosized MCM-22 has been synthesized for use as a support in MDA, and it showed improved methane conversion, benzene yield, and catalyst durability.[38] The pore sizes and structures within the zeolites dictate what can pass through and what is trapped inside the zeolite. Larger pore sizes are more resistant to coke formation and accumulation, but are less selective as larger products (such as naphthalene) can easily pass through these pores.[6] Another important factor is the acidity of the zeolite and the active sites within its structure. These can be tuned with silicon-to-aluminum ratio (SAR) variation, but some studies have introduced mesopores into zeolite structures

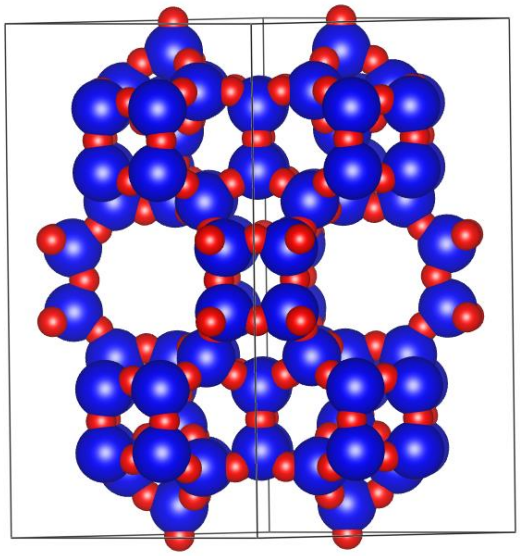

or selectively etched away parts of the zeolite to tune both its pore structure and acidity.[39] By changing the zeolite structure to a mesoporous zeolite, selectivity for coke has been shown to decrease; however,the synthetic methods for these zeolites are currently unrealistic for commercialization. A recent study by Martínez and Peris showed that when the protons of H-ZSM-5 were partially exchanged for Na^+, Cs^+, Ca^{2+} or Mg^{2+} the strength and density of the acid sites could be tuned. The loss of strong acid sites led to lower activity towards methane conversion, but benzene selectivity was improved and catalyst decay rates were decreased in the case of sodium and cesium. The addition of calcium and magnesium produced similar results, though not as pronounced as with the alkali cations. Each was successful at suppressing coke formation, thus extending the relative catalyst lifetime; however, exchanged catalyst activity was still lower than on unmodified Mo/ZSM-5.[40]

The molybdenum catalyst is typically introduced into the zeolite via a wet impregnation process followed by calcination, which forms Mo oxide on the zeolite surface. To activate the catalyst, it must be carburized to form molybdenum carbide before any desired products are produced. Generally, this is done through *in situ* carburization as methane gas is passed over the oxide catalyst at reaction temperatures (973-1023 K), which completes the carburization of the catalyst within a few hours. During carburization, the molybdenum (Mo^{6+}) is partially incorporated into the zeolite structure at the Brønsted acid sites, deactivating those sites. Only about 60-80% of the Mo^{6+} is incorporated into the Mo-carbide structure, at which point a quasi-steady state of methane conversion and benzene yield is reached. Molybdenum oxide species still coexist after carburization, especially within the narrow pores of the zeolite due to mass transport limitations.[24] After carburization initiation, molybdenum carbide sites begin to convert CH_4 into ethylene and hydrogen, which then react on the acid sites to form aromatics.[32] Additionally, throughout the process coke is forming within the pores. All of these factors lead to relatively low catalyst activity and short time-on-stream conversions of methane. Understanding the process by which Mo is carburized and further understanding the coking mechanism of the MDA reaction could lead to improved catalyst activity and, eventually, commercialization of this technology. However, there is no consensus on the actual structure of the molybdenum carbide catalyst due to its dependence on individual reaction conditions.

2.3. Biomass Conversion Chemistry

The third type of chemistry that often employs carburized catalysts is biomass conversion. In biomass conversion the feedstock fuels include a wide variety of oxygenated hydrocarbons and aromatic compounds generally derived from pyrolysis, gasification, liquefaction, or hydrolysis of biofeedstocks.[41] However, each type of biomass conversion chemistry is complex and involves input and output of carbon, therefore; obstacles arise with coking and the formation of undesirable side products like tars and other impurities. The main biomass conversion reactions include hydrolysis, dehydration, isomerization, reforming, aldol condensation, hydrogenation, oxidation, and hydrogenolysis. Hydrolysis, dehydration, isomerization, oxidation, and aldol condensation are often carried out at lower temperature (≤400 K). Hydrogenolysis and hydrogenation are done at higher temperatures (470 K), and aqueous phase reforming at even higher temperatuers (500 K). Most of these processes are carried out at relatively low pressures (<50 atm), but higher pressures are occasionally required for water to remain in the liquid state.[42] In hydrolysis, glycosidic bonds between sugar units are

cleaved resulting in the formation of simple sugars. Dehydration reactions convert sugars into furan compounds. Isomerization is useful for converting glucose to fructose. Reforming is typically used to produce hydrogen, which can then be used in applications like hydrogen PEM fuel cells and hydrogenation reactions. Aldol condensation reactions form C-C bonds with the help of an acid or base catalyst at relatively mild temperatures. Hydrogenation takes place over a metal catalyst to saturate C=C, C=O, and C-O-C bonds. Oxidation is carried out over supported metal or metal oxide catalysts as well. Finally, hydrogenolysis of C-C or C-O bonds takes place under H_2 gas, also with supported metal catalysts.[42] The resulting products in biomass conversion often include syngas, but are more complicated than FTS chemicals as they contain hydrocarbons, aromatics, water vapor, some sulfides, and even trace inorganic materials.[41] This makes separation of the final products more complicated than FTS and MDA but also allows for a wider range of products. Generally, biomass conversion will follow these steps:

$$\begin{gathered}\text{biomass} + \text{oxidant}\ (O_2, H_2O) \rightarrow \\ CO, H_2, CO_2, H_2O, CH_4 + \text{hydrocarbons} \rightarrow \\ \text{tar} + \text{char} + \text{ash} \rightarrow \\ H_2S + HCN + NH_3 + HCl + \text{sulfur species}\end{gathered}$$

Eq. 4

Also, as in FTS, water can play an important role in the overall chemistry. Water is necessary for steam reforming to produce CO and H_2 or WGS as it reacts with CO to form CO_2 and H_2 (Equation 2). Dry reforming is also possible where the hydrocarbons interact only with CO_2 to form CO and H_2. By selectively tuning these conditions many different chemical pathways are accessible. As with FTS and MDA reactions, the catalysts used in biomass conversion are thoroughly researched and provide substantial information on improving processes to achieve improved yields and longer time-on-stream. While almost all transition metals have been studied as possible catalysts for these reactions including Fe, Mo, Rh, and Pt; Ni appears to be the most commonly used catalyst.[41] For commercialization, less expensive, more earth-abundant metals are desirable, though precious metals have historically shown excellent activity. Biomass conversion catalysts usually include a promoter such as Mg or CeO_2 and a support material like silica or zeolites, each of which affect the overall activity of the catalyst.[41]

Nickel oxide is one of the most active catalysts for biomass conversion, but activation curves are observed to be similar to those seen for Mo oxide during the initial time-on-stream for MDA. This suggests that Ni oxide may undergo partial *in situ* carburization, or at least reduction to nickel metal, before the formation of desired products.[43, 44] This can be done *in situ* with the biomass pyrolysis vapors, or can be performed *ex situ* with hydrogen gas mixtures.[43] It is also observed that molybdenum oxide biomass catalysts must first become carburized before conversion occurs.[45, 46] Some research indicates that it may be the interaction between the oxide and carbide form of the metal catalysts that most efficiently reacts with the biomass.[47-50] Many reaction pathways also specify that surface carbon plays a role in the formation of final products, meaning that either the metal or the support is carburized during biomass conversion. Coking itself is a form of carburization as the hydrocarbons are activated on the catalytic surface; the carbon dissociates and begins to accumulate on the catalyst surface instead of forming desirable products.[51] As surface carbon forms, it nucleates and arranges into even larger carbon deposits that eventually lead to catalyst deactivation.[41] In some cases such as with pure Ni, coke deactivates the catalyst leading to decreased activity over time.[52] The stability of transition metal carbide catalysts employed in liquid-based reactions

for biomass conversion has been recently reviewed by Macedo *et al*.[53] The type of metals, promoters, and supports used as biomass conversion catalysts affect coke formation and are heavily influenced by *in situ* carburization.

3. Mechanisms of *In Situ* Carburization

Carbide catalysts can be formed from a variety of starting materials, the most common of which are metal oxides and pure metals. The metal is obtained from metal salts such as ammonium heptamolybdate, ammonium paratungstate, or iron or nickel nitrates that are dissociated, dried, and calcined in air to form the corresponding metal oxide.[54] If a support material is used, these metals are introduced via an incipient wetness preparation followed again by drying and calcination. The resulting transition metal oxides may be of different oxidation states depending on application and synthetic procedures and are often first reduced before carburization. This metal oxide precursor influences the types of carbide catalysts that can be formed, and the reduction steps influence the time scale of the reaction.

3.1. Fischer-Tropsch Catalysts

Iron oxide precursors that are reported as FTS precursors include hematite (α-Fe_2O_3), magnemite (γ-Fe_2O_3), magnetite (Fe_3O_4), FeO, and FeOOH.[14] During typical FTS reaction conditions iron oxide undergoes reduction (H_2 gas) via the following steps: α-Fe_2O_3 → Fe_3O_4 → FeO → α-Fe.[55] These species can be carburized to create active sites for FTS. While studying the carburization process of iron during FTS, Janbroers *et al*. discovered that their oxide precursor consisted of small oxide particles in the hematite phase.[56] This species was reduced to magnetite, during which there was sintering of the particles, before carburization. The first step of iron activation during FTS involves the transformation from α-Fe_2O_3 to Fe_3O_4 regardless of the carburizing gas mixture. Li *et al*. synthesized iron oxide powder catalysts with different promoters (Zn, K, Cu) for FTS.[54] Each powder consisted of iron oxide in the form of Fe_2O_3 which underwent reduction and carburization during initial FTS heating as follows: reduction of Fe_2O_3 at 543 K to Fe_3O_4, then reduction/carburization of Fe_3O_4 to form Fe_xC (where x equals 2.5 or 3) from 543-723 K. The promoters had no influence on the first reduction step of the iron oxide which was required before carburization could occur; however, they did affect the further reduction of the iron oxide and its carburization behavior. The next step is more dependent on the gas used, and leads either directly to iron carbides (CO or CO/H_2) or further reduction to metallic iron followed by carburization (H_2).[57, 58] Vo *et al*. started with a MoO_3 precursor on an alumina support, obtained by calcination of aqueous ammonium heptamolybdate salt on the support material, which was reduced to an oxycarbide species before further carburization.[59]

Iron carbides are generally formed from iron oxide by *in situ* carburization with reactive gas, CO and H_2. Iron carbides do not form perfect geometrical lattices like early transition metal (group IV, V, VI) carbides, but have distorted lattices where carbon atoms can interact with other carbon atoms directly.[14, 60, 61] These carbon-carbon interactions lead to catalytic performances unique to that of early transition metal carbides, and the free carbon helps tune the chemical environment of the iron to make it an effective catalyst for FTS chemistry. Some iron carbides have stable structures (graphite), but more often metastable carbides like $Fe_{2.5}C$ and Fe_3C are formed (Figure 3).[14]

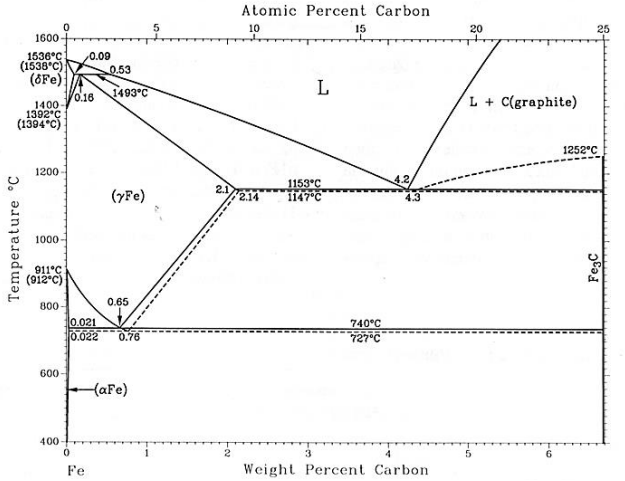

Figure 3. Fe-C diagram from 0 to 25 atomic % carbon. The stable graphite phase is in the upper right portion of the equilibria graph, and metastable cementite (Fe_3C) in the middle.[60]

Iron-carbon binary systems are never completely thermodynamically stable, but play important roles in carburization and catalysis during FTS.[61] This makes characterization of the active iron carbide species difficult, especially since they are formed *in situ*. Other published work suggests that χ-Fe_5C_2 is the active phase in FTS, which shows high activity for CO activation and chain growth.[47] Li *et al*. used powder X-ray diffraction to characterize their iron carbide active phase as a mixture of $Fe_{2.5}C$ and Fe_3C.[54] Carbon chemical potential can be used to explain iron carbide transformations during FTS reactions. The most commonly observed forms of iron carbides are ε-Fe_2C, χ-Fe_5C_2, and ɵ-Fe_3C due to their high stability, low deformation energy of the hcp lattice, and high stability at low carbon chemical potential conditions, respectively.[47] An early study by Amelse, Butt, and Schwartz found that α-Fe_2O_3 was reduced to α-Fe under H_2 before being completely carburized in CO/H_2. This carbide catalyst was in the ε' ($Fe_{2.2}C$) form as opposed to more commonly reported χ or ε form, perhaps due to support interaction with silica gel.[62]

In FTS, the carburizing gas mixture is CO and H_2. At typical reaction temperatures, iron oxide is readily converted to the active iron carbide species.[14]

$$Fe_xO_y + yH_2 \leftrightarrow xFe + yH_2O$$
$$Fe_xO_y + yCO \leftrightarrow xFe + yCO_2$$
$$CO \rightarrow C + O \; over \; active \; surface \; site$$
$$yC + xFe \rightarrow Fe_xC_y \quad \text{Eq. 5}$$

At low reaction temperatures, 450-500 K, iron oxide reduction can take place; only when temperatures begin to approach FTS reaction temperature (>500 K) does carburization occur.[54] The crystallinity of iron and molybdenum carbides and the degree of carburization can be tuned with reaction temperature, carburizing gas mixture, structure of the metal oxide precursor, and reaction time.[63] Iron carbon core-shell nanostructures have been formed *in situ* during FTS of iron supported on biochar, where biochar is the carbon source for the carbide formation. These nanoparticles consisted of α-Fe, Fe_3C, and graphite.[64] In another example, when iron is exposed to a H_2 gas atmosphere, it is reduced from Fe_3O_4 directly to metallic Fe. However, when the carburizing gas is CO, iron carbides form from the same iron oxides.[65] Changes have been made to the basic processes in order to make them more industrially viable or attempt to improve the product formation. Low temperature FTS (Sasol process) produces longer chain hydrocarbons compared to the higher temperature process.[66] Molybdenum catalysts have also been employed as alternative catalysts during the FTS process. Vo and Adesina obtained the α-MoC_{1-x} carbide through a typical wet impregnation method on alumina.[59] This catalyst was more tolerant of higher CO partial pressures during FTS than Co and Fe catalysts due to CO adsorption on unsaturated Mo-carbon sites.

3.2. Methane Dehydroaromatization Catalysts

Many different molybdenum oxide species are formed *in situ*; however, the actual oxide species are not all agreed upon in the literature. Different oxidation states are thought to be present during this reduction stage that precedes carburization, though almost all researchers agree that at some point MoO_3 is reduced to MoO_2 during carburization. Ma *et al*. discovered that metal-doped molybdenum carbides could be formed from salt precursors, but observed many different intermediate Mo oxide species.[67] The main process was reduction of MoO_3 to MoO_2 followed by carburization, but they also observed some MoO_xC_y species before full carburization. These same observations were made by Hanif in 2002 with non-doped Mo species.[68] However, through chemical modeling, it was discovered that Mo species supported on zeolites are first reduced from MoO_3 to Mo_2O_5, which can be directly carburized.[69] More recently, Gao *et al.* determined that nanostructured molybdenum oxide formed agglomerates during carburization, and that these could be converted back to the oxide form with the introduction of oxygen.[70]

The active phase of molybdenum carbide is often specified as Mo_2C, but the understanding of the exact nature of these Mo carbides has changed over time. The β-Mo_2C surface can be terminated with either Mo or C atoms.[71] Hanif *et al*. found that the ramp rate during the initiation of carburization changed the temperature at which Mo oxide became fully carburized.[68] Many studies found the β-Mo_2C to be the active species after carburization;[67, 72-75] with other Mo carbide species often observed in these studies. Density functional theory has shown that the β-Mo_2C(001) surface has similar carbon reactivity to group VIII/IX metals and is more reactive towards oxygen and hydrogen species than group VI metals.[76] Others suggest that Mo oxide is never fully carburized and instead Mo_2C and MoO_xC_y catalysts are both present and work in tandem as the active species.[77] The Mo_2C surface can form subsurface oxides, hydrides, or oxycarbides at typical reaction conditions.[76] Lee *et al*. determined that the active phase of Mo carbide was either β-Mo_2C (hexagonal close-packed) when carburized directly or with a metallic intermediate, or α-MoC_{1-x} (face-centered cubic) when prepared through a nitride intermediate, with x being about ½.[78] Matus *et al*. concluded that the molybdenum carbide species formed outside the pore structure cannot be the active site as it is covered by 2-3 nm of graphitic carbon. Instead, it is the molybdenum within the pore channels that is active since it is not as easily carburized and is in close proximity to the acid sites of the zeolite.[29] Additionally, support properties can be affected by the harsh conditions typical of these reactions. Increasing the calcination temperature above 1023 K of 2 wt% Mo/HZSM-5, while holding all other MDA reaction conditions constant, was found to decrease surface area, methane conversion, and benzene production due to dealumination of the zeolite.[79] If carburization of MoO_3 occurs prior to the MDA reaction, benzene formation temperature is lowered from above 1000 K to 847 K as compared to the *in situ* carburized catalyst.[37] Mo/zeolite catalysts prepared on Y-zeolite were found to be much more stable towards benzene hydrogenation at lower temperatures when reduced with a methane/hydrogen mixture rather than with pure hydrogen, as methane increased the available number of coordinatively unsaturated sites on the catalyst.[73]

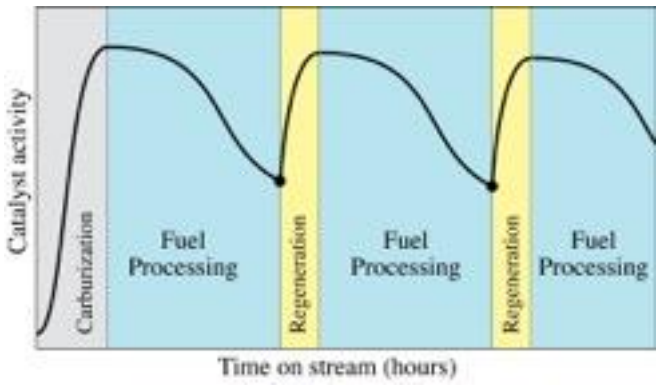

Figure 4. Methane dehydroaromatization catalyst activity as a function of time-on-stream during the reaction. Products are formed during the fuel processing period.[75]

In MDA, and other chemistries involving molybdenum carbide catalysts, the most common carburizing gas is methane, or a combination of methane and hydrogen. Typically, carburzation of the catalyst is observed, followed by a fuel processing period before catalyst deactivation (Figure 4). Reaction temperatures for Mo carbide also tend to be higher than some FTS temperatures, ranging from 973-1123 K.[29, 32] An early study of molybdenum carbide catalysts by Lee *et al*. compared carburization methods to overall catalyst performance.[78] The first method was a reduction of the Mo oxide in H_2 followed by carburization with a 20% CH_4/H_2 mixture; the second method was direct reduction/ carburization in the methane/hydrogen mixture; the third method was to use ammonia as the precursor for nitridation followed by carburization in the methane/hydrogen gas. The catalysts were tested for benzene hydrogenation, where the two catalysts not prepared by direct carburization initially performed better. However, they deactivated quickly with time-on-stream and increased reaction temperatures. The catalyst formed by direct carburization showed low activity throughout the reaction profile, but did not deactivate as quickly as the other catalysts. Most commonly, MoO_3 was reduced to MoO_2 followed by carburization via CH_4 to form MoC_x species, which varied depending on reaction conditions.[31] Iron has also been used for methane dehydroaromatization, and its incorporation into a silica matrix allowed for activation of methane and formation of methyl radicals that increased the selectivity towards ethylene. Additionally, this catalyst was able to convert up to 48% of the methane reactant gas with a hydrocarbon selectivity (benzene, ethylene, and napthalene) of 99% at 1363 K and 21,400 space velocity ml g^{-1} h^{-1}. However, most of the methane was converted to ethylene or naphthalene, with benzene yields remaining fairly low.[3]

3.3. *Biomass Conversion and Related Processes Catalysts*

Many different metals may be employed for biomass conversion reactions. When Mo carbide was used for biomass conversion, the oxide was first reduced at lower temperatures then carburized once higher temperatures were achieved. This catalyst was effective for steam reforming of biomass tar.[45] When $Mo(CO)_6$ was used as the catalyst precursor it was thermally decomposed to Mo_2C in H_2 above 800 K, but the carbide was destroyed and Mo metal formed at conditions above 970 K. In this study, the Mo_2C/Al_2O_3 catalyst was able to chemisorb twice as much CO as the Mo/Al_2O_3 catalyst supporting the hypothesis that the carbide phase is the active phase for CO hydrogenation.[80] York and coworkers were able to produce a partially carburized molybdenum oxide (which they denoted as MoO_3-carbon modified) by carburizing commercially available MoO_3 under *n*-heptane and H_2 gas at 623 K.[77] In a recent study by Kaewpanha *et al*. biomass char was used as the support material for the molybdenum catalyst.[45] The char used as the support material was also the carbon source required for carburization of Mo to

Mo_2C at temperatures above 873 K, demonstrating an effective way to form active catalyst in a single *in situ* step. This biomass supported catalyst was found to work well for steam reformation of tar.

Nickel is the most common metal catalyst for biomass conversion and exists as both metallic Ni and Ni oxide. It also has important interactions with promoters and supports, which are often metal oxides.[41] In one study, Ni/ZSM-5 was used to upgrade pine pyrolysis vapors to aromatic hydrocarbons. The authors found that pre-reduced (*ex situ*) Ni/ZSM-5 initially performed better than ZSM-5 alone or NiO/ZSM-5, but deactivated quickly. NiO/ZSM-5 was reduced *in situ*, and initially showed activity similar to bare ZSM-5, but eventually reached activity that was the same as the Ni/ZSM-5 catalyst, suggesting the nickel reaches the same end state, regardless of pre-treatment.[43] Finding the optimal reduction temperature must be considered for each reaction, as below a certain temperature the reduction will not yield an effective catalyst, but too high a temperature can cause sintering. In the case of reduction of NiO in H_2 gas on an alumina support, Cheng *et al*. found the optimal reduction temperature to be 873 K.[44]

Nickel carbide is not often observed during biomass conversion reactions, but there is evidence that it works synergistically along with carbon supports after reduction. Ni/C has been used to form aromatic hydrocarbons from lignin, which is often the most difficult biomass precursor to break down and is typically treated as waste.[81] It has also been observed that Ni metal on NiC species exhibits superior catalytic properties when compared to Ni on carbon. For the hydrogenation of chloronitrobenzene, NiC/Ni carbon nanofibers were able to convert 97-100% of the starting material, whereas the Ni on carbon catalyst converted only 67%. The formation of carbon nanofibers and incorporated nickel carbide could only occur after the initial reduction of Ni^{2+} to Ni^0 by carbon containing precursors.[82] In another carbon nanofiber growth study with nickel as the growth substrate, it was found that nickel can be present in three stages during the growth process: Ni_3C at 573 K, composite formation of Ni-Ni_3C_{1-x} at 673-773 K, and Ni metal at 873 K. They also note that no stable nickel carbides can be formed, but that metastable species are often present at lower temperatures (below 1373 K).[83] Ni-W_2C supported on activated carbon has been shown to be comparably active to noble metal catalysts in hydrocracking of woody biomass to form ethylene glycol.[84] Nickel metal can be carburized to form Ni_3C which occurs in small amounts during methanation with CO gas as the reactant at 538 K. [85]

3.4. Other Processes Utilizing Carbide Catalysts

Other metal catalysts are active in their carbide form and are typically created during the progress of the reaction. Vogel used *in situ* XRD to monitor the formation of palladium carbide catalysts when Pd metal is supported on carbon. Though it is often thought that carbon formation is solely in the form of coke deposits, it was shown that at 623 K the Pd lattice becomes saturated with carbon. The distribution of the carbon throughout the nanoparticles is not homogeneous, and they can also form PdC_xH_y structures when exposed to hydrogen after carburization.[86] Often studied due to its similar catalytic properties to Pt is tungsten carbide, which can be formed *in situ* under carburization conditions similar to Mo_2C. One early study reported the formation of WC during reduction and carburization of WO_3 powder with CH_4/H_2 gas at high temperatures. The catalytic properties for hydrogenolysis were shown to be similar to Ru, Ir, and Ni for cracking reactions.[87] Since the discovery that WC behaves similarly to precious metal catalysts, others have worked to prepare bulk tungsten carbide[88] and supported tungsten

carbide[89] as lower cost replacements to noble metals. Ni(111) is used as a substrate to grow graphene as its lattice structure closely matches 2D graphene. During the graphene growth, an intermediate layer of Ni_2C is formed. The graphene grown on the carbide surface exhibits different electronic properties from Ni(111) templated graphene, and prevents oxidation to NiO.[90] Detonation spraying is used in coating deposition technology, and relies on the complete combustion of the fuel (acetylene) to produce coatings without solid carbon deposits. When nickel is incorporated in this process, it was found that *in situ* carbon dissolved in the molten nickel, forming metastable hcp-Ni and fcc-Ni. The carbon stabilizes the nickel in these lattice structures, and prevents immediate oxidation to NiO.[91] Carburization of molybdic acid in CH_4/H_2 resulted in hexagonally arranged Mo_2C after Mo_4O_{11} was first reduced to MoO_2 then Mo metal.[92] Adzic and coworkers observed the process of Mo carburization via *in situ* time resolved synchrotron XRD as the decomposition of ammonium heptamolybdate on a carbon support occurred.[72] They were able to follow the process using thermodecomposition measured by thermogravimetry-differential thermal analysis. (TG-DTA). During the initial stages of weight loss, the ammonium heptamolybdate decomposed to form MoO_3. It was found in the carbon supported sample that MoO_3 was reduced to MoO_2 around 788 K and then carburized. Molybdenum carbide species have also been used as support materials for other catalysts. In a study by Berhault *et al*. MoS_2 samples were carburized to create structural carbon that stabilized the catalyst.[93] They found that the bulk MoS_2 structure remained intact, but that the support carbon was of a carbide nature with small amounts of amorphous carbon. This support structurally modified the catalyst in a way that increased the activity when compared to Al_2O_3 supported molybdenum sulfide.

3.5 Deactivation and Regeneration of Carbide Catalysts

In situ catalytic processes require regeneration steps for the catalysts involved after deactivation. Carbide catalysts, especially, tend to deactivate quickly due to reactions with carbon and oxygen containing gasses. The cost of regenerating catalysts during these reactions has a large overall effect on process economics.[94] General types of catalyst deactivation have been reviewed extensively by Bartholomew, Forzatti, and Leitti, with iron carbide being studied in depth by de Smit.[14, 95, 96] One of the most prominent deactivation mechanisms is by coking of the catalyst; after the metal carbide is formed, carbon continues to deposit on the catalyst, coking the surface and preventing access to active sites.[97] In addition to covering the surface of the catalyst, coke can block the pore openings of supported catalysts, especially in structures with subnanometer pores such as zeolites.[98] While the metal carbide is active for catalysis, subsequent carbon layering tends to form unreactive graphitic carbon, deactivating the catalyst. Nickel catalysts can also be deactivated by growth of carbon “whiskers” that detach Ni from the support, or by pyrolytic type carbon during cracking reactions, though Ni(III) is more resistant to coke formation.[99] An effective regeneration method for this type of deactivated catalyst is to include some oxidant in the regeneration gas stream, such as steam, O_2, or CO_2. However, the same oxidants can cause overoxidation, especially in iron carbide, to form inactive Fe_3O_4; often this occurs *in situ* as H_2O is formed during high conversion periods of FTS.[14, 100, 101] Hydrogen gas can also be used to regenerate these catalysts with the added benefit that recarburization is not always required to reach the active form of the material. Choi et al. determined that catalyst surface coking was the major source of deactivation during bio-oil hydroprocessing. They examined regenerating their Mo_2C

catalyst *in situ* with H_2 gas at 698 K, and were able to produce sufficient quality upgraded oil after each regeneration step for 4 active runs.[100] Pour et al. observed that the selectivity for light hydrocarbon products during FTS over Fe/ZSM-5 increased with reaction time. They attributed the deactivation of their catalyst to phase changes in the iron carbide, coking of the iron catalyst, and significant coking of the zeolite. They regenerated their catalyst with O_2/N_2 mixture at 573 K, but found that while the coke on the iron carbide surface could be completely removed, this treatment was not successful in decoking the zeolite.[98] Another obstacle to consider during these reactions is poisoning of the catalyst, which takes place at ppb levels in Fe, Ni, and Co catalysts by H_2S gas. Sulfur containing gases naturally occur in industrial synthesis gas as well as in byproducts of biomass conversion. Poisoned catalysts cannot be regenerated, therefore, keeping the amount of poison content in the feed at low levels is highly important.[96] One final deactivation process that must be considered is sintering of the metal particles. Sintering can occur on both unsupported and supported catalysts, and the growth of the active metal particles can lead to deactivation through a loss of total active sites during the reaction. The reaction temperatures of FTS, MDA, and biomass conversion tend to be high (around 1000 K), leading to this type of deactivation. During the decomposition of methane over a Ni/SiO_2 catalyst, Takenaka et al. first observed sintering of the Ni particles almost immediately after they were put in contact with methane. Additional deactivation was caused by the deposit of coke and the formation of some nickel carbide species.[102] One way to limit sintering is to choose a support with which the metal will form strong metal-support interactions, imparting greater stability.

4. Improvements to the Processes

4.1. Alternative Carburization Gas Mixtures

Most carburizing gases are composed of the reactive mixture used for the specific catalytic reaction, CO and H_2 or CH_4; however, some studies have analyzed the effects of using different gases to form metal carbides. In a study conducted by Chen *et al*. molybdenum carbide catalysts were formed by *in situ* carburization of ammonium molybdate on carbon nanotubes and carbon black without any additional carbon gas source.[72] In order to form the catalyst precursor, ammonium molybdate and the carbon source were mixed in water followed by drying. Carburization took place under Ar flow at 1073 K. During carburization the Mo salt decomposed to form α-MoO_3 followed by the formation of Mo_8O_{23} and Mo_4O_{11} intermediates as determined by *in situ* time-resolved synchrotron XRD. Finally, around 688 K, MoO_2 was obtained prior to carburization of the Mo oxide. This study concluded that Mo_2C nanoparticles formed from this solid-state reaction are anchored into the carbon supports. Vo and Adesina used a carburizing mixture of $5H_2$:$1C_3H_8$ after typical wet impregnation of ammonium heptamolybdate on an alumina support. [59] This resulted in complete carburization of MoO_3 to form α-MoC_{1-x} and β-MoC_{1-x} phases of the catalyst along with some Mo oxycarbide species. In a 2007 study by Wang *et al*. β-Mo_2C was formed in a single-step carburization on an alumina support.[103] The precursor ammonium molybdate salt contained hexamethylenetetramine (HMT) and was either mechanically mixed or the aqueous mixture was evaporated after mixing with the support. The mixture was dried and then heated under argon at temperatures near 973 K to form the Mo carbide. They found that the best products were obtained when the precursors were thoroughly mixed, enough HMT was in the mixture for an adequate carbon source, and with higher heat treatment.

In a study on the formation mechanism of molybdenum carbides, Green and coworkers used both conventional carburization gas (methane) as well as ethane balanced with hydrogen.[68] They found that the behavior of hydrogen in both systems was similar, and both reduction and carburization occurred with either gas. However, ethane was found to be more active in the reduction process, and the transitions occurred at lower temperatures. Additionally, the Mo carbide particles formed with ethane as the carburizing gas were smaller and had greater surface area than the corresponding methane carburized materials. Another Green study in 2002 employed acetylene (C_2H_2/H_2) as the carburizing agent; MoO_3 was heated under acetylene flow at temperatures ranging from 723-903 K.[104] At the low temperature end, MoO_3 was reduced to MoO_2 but no detectable Mo carbide structures were formed. Less MoO_2 was observed in the sample heated to 773 K, but still no carbide was formed. At the higher temperatures, no Mo oxide remained and MoC_{1-x} was the phase of carbide observed for these catalysts. It was found that compared to other carburizing gases, acetylene produces the smallest Mo carbide crystallites. Compared to most conventional *in situ* carbide preparations, this method works well at lower temperatures, producing catalysts active for methane partial oxidation to syngas.

4.2. Metal Promoters and Alloys

One of the most promising routes for increasing catalyst lifetime and activity is to combine other metals with the active catalyst. These metal combinations can assist in different aspects of the catalysis such as the activation process, the carburization process, reduction of coke formation, or extending catalyst lifetime. It has been shown that a FeRu alloy can be used for FTS without the formation of any carbide structure within the catalyst. This catalyst requires no activation period but suffers from rapid deactivation.[18] Other FTS promoters include Cu, K, and Zn. Copper promotes reduction of the iron oxide species, potassium enhances CO adsorption thus increasing carburization activity, and zinc prevents iron oxide particles from sintering and helps maintain higher surface areas.[105] During an *in situ* TEM study, no carburization occurred on plain Fe_3O_4 samples with CO gas, but once K was introduced as a promoter, iron carbide formation took place without extra carbon deposition in the form of coke since the CO dissociates and carbon dissolves into a metallic iron phase.[56] It has also been found that potassium promoted iron catalysts have relatively low methane selectivity, which is the least desired product in FTS, though the mechanism by which K enhances the selectivity is still unknown.[16] In a study of how promoters affected carburization during FTS, researchers found that the rate of carburization increased in the following order: no promoter < Li < Na < K ≈ Rb ≈ Cs. The better promoters were found to decrease the reduction temperatures for the catalyst. After reduction of the metal catalysts, carburization takes place relatively easily.[54, 106] Other metal promoters that resulted in higher amounts of reduction and carburization under CO atmosphere include Zn and Al. These catalysts also had higher selectivity for C_5+ hydrocarbon products.[54, 107]

Molybdenum/ZSM-5 catalysts for methane dehydroaromatization were studied with Fe and Fe-Zn promoters. With iron as the only promoter, the rate of benzene formation increased by 35% over a 12 hour time period, whereas the catalyst with only zinc as the promoter showed the same activity as the unpromoted Mo catalyst after 3 hours. Interestingly, when Mo/ZSM-5 contained both Fe and Zn promoters, benzene formation dropped by 31% due to the formation of high temperature coke deposits.[108] Nickel modified Mo_2C has been used as a catalyst for dry reforming of methane by incorporating

the nickel species at the beginning of the metal oxide synthesis. The products of this process are CO and H_2 in suitable ratios for FTS. The nickel was found to assist in the reduction of the molybdenum oxide by decreasing the required temperature by 100 K. During catalysis of CH_4/CO_2 mixtures, Mo_2C was found to convert only 7 and 10% CH_4 and CO_2, respectively, whereas the Ni-Mo_2C catalyst achieved conversions of 82 and 93%. Nickel is thought to both improve the reducibility of Mo oxide as well as aid in the dissociation of methane on the catalyst surface, thus enhancing catalytic activity.[109] The final carbide phase of Mo was found to be β-Mo_2C despite changing the promoter metal from Cu to Ni or Co, but each catalyst behaved differently during CO_2 hydrogenation (Figure 5).

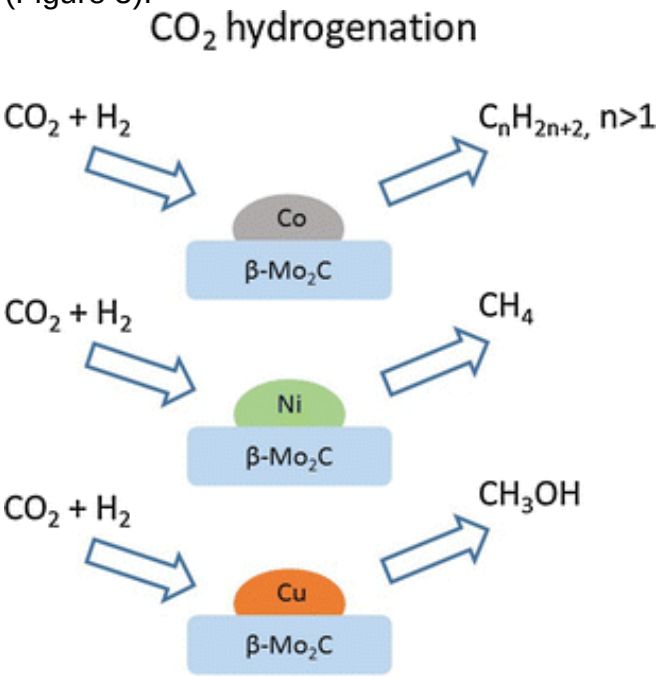

Figure 5. Reaction pathways and products for carbon dioxide hydrogenation over different metal-doped molybdenum carbide catalysts.[74]

Nickel/molybdenum nanoparticles dispersed on the Mo_2C surface show carbon conversion of 100% and hydrogen selectivity of up to 95% during the partial oxidation of surrogate biodiesel to syngas, a significant improvement from only 70% hydrogen selectivity with molybdenum carbide alone.[110] Nickel has also been used as a promoter for tungsten carbide catalysts for biomass conversion applications. It was found that the nickel increased selectivity for cellulose conversion to ethylene glycol when compared to Pt/Al_2O_3 and Ru/C catalysts. As with Mo, the nickel lowered W_2C formation temperatures by decreasing the required energy for tungsten reduction.[111] Nickel has also been used in a tandem catalytic system with tungsten carbide for the conversion of glucose to ethylene glycol by a retro-aldol reaction followed by hydrogenation.[112] Ma *et al*. discovered that the type of metal doped into the catalyst determined its final carburized form, for example doping with Fe, Co, or Ni formed the common β-Mo_2C species.[67] In the case of Pt doping, α-Mo_2C was formed along with β-Mo_2C, and the amount of α phase increased with Pt doping amount. The Pt doped catalyst was especially active for steam reforming of methanol even at low temperatures as it had the highest surface area and longest catalyst lifetime due to strong metal-support interactions of Pt with the Mo carbide. Nickel/Mg/Al catalysts were compared to Ni-Fe/Mg/Al catalysts for the steam reforming of biomass tar. The steam reforming of toluene and benzene over the alloyed Ni-Fe catalyst had higher turnover frequencies (TOFs) than the Ni catalyst, perhaps due to surface carbide stabilization on the Fe during hydrocarbon adsorption. In addition, carbon deposition on the catalyst was suppressed by Fe incorporation.[113]

5. Conclusion

Catalysts employed in Fischer Tropsch synthesis, methane dehydroaromatization, and biomass conversions are typically transition metal carbides that form *in situ*. Each of these chemical processes is a viable alternative to conventional petroleum derived

fuel production, and they are considered green chemistry routes. Many of the most efficient metal catalysts are abundant in nature, and thus cost efficient alternatives to precious metals. The catalyst species present after carburization depend on the metal oxide precursor and reaction conditions such as temperature and carburization gas, making the determination of the active phase difficult despite numerous studies. The incorporation of other metal dopants can lead to favorable reduction and carburization properties during catalysis.

Acknowledgements

The authors would like to thank CoorsTek, Inc. for supporting this work and research in MDA. BGT would like to thank the National Science Foundation grant number 1508728 for financial support for completion of this review.

Keywords: Metal carbide • in situ • Fischer-Tropsch • methane dehydroaromatization

[1] P. T. Anastas, M. M. Kirchhoff, T. C. Williamson, *Appl. Catal. A.* **2001**, *221*, 3-13.
[2] O. James, O., B. Chowdhury, M. A. Mesubi, S. Maity, *RSC Adv.* **2012**, *2*, 7347-7366.
[3] X. Guo, G. Fang, G. Li, H. Ma, H. Fan, L. Yu, C. Ma, X. Wu, D. Deng, M. Wei, D. Tan, R. Si, S. Zhang, J. Li, L. Sun, Z. Tang, X. Pan, X. Bao, *Science* **2014**, *344*, 66-619.
[4] M. E. Dry, *Catal. Today* **2002**, *71*, 15.
[5] A. G. Judd, M. Hovland, L. I. Dimitrov, S. Garcia Gil, V. Jukes, *Geofluids* **2002**, *2*, 109-126.
[6] S. Ma, X. Guo, L. Zhao, S. Scott, X. Bao, *J. Energy Chem.* **2013**, *22*, 20.
[7] P. V. L. Reddy, K.-H. Kim, H. Song, *Renew. Sustainable Energy Rev.* **2013**, *24*, 578-585.
[8] S. Majhi, P. Mohanty, H. Wang, K. K. Pant, *J. Energy Chem.* **2013**, *22*, 543-554.
[9] J. C. Serrano-Ruiz, J. A. Dumesic, *Energy Environ. Sci.* **2011**, *4*, 83-99.
[10] G. Centi, E. A. Quadrelli, S. Perathoner, *Energy Environ. Sci.* **2013**, *6*, 1711-1731.
[11] (Ed.: **BASF**), Germany, **1913**.
[12] F. Fischer, H. Tropsch, *Brennstoff-Chemie* **1923**, *4*, 193-197.
[13] F. Fischer, H. Tropsch, Germany, **1925**.
[14] E. de Smit, B. M. Weckhuysen, *Chem. Soc. Rev.* **2008**, *37*, 24.
[15] H. Schulz, *Appl. Catal., A.* **1999**, *186*, 3-12.
[16] J. Yang, W. Ma, D. Chen, A. Holmen, B. H. Davis, *Appl. Catal. A.* **2014**, *470*, 11.
[17] Q. Zhang, K. Cheng, J. Kang, W. Deng, Y. Wang, *ChemSusChem* **2014**, *7*, 14.
[18] J. W. Niemantsverdriet, A. M. Van Der Kraan, *J. Catal.* **1981**, *72*, 385-388.
[19] B. Ernst, A. Bensaddik, L. Hilaire, P. Chaumette, A. Kiennemann, *Catal. Today* **1998**, *39*, 329-341.
[20] G. L. Bezemer, J. H. Bitter, H. P. C. E. Kuipers, H. Oosterbeek, J. E. Holewijn, X. Xu, F. Kapteijn, A. J. van Dillen, K. P. de Jong, *J. Am. Chem. Soc.* **2006**, *128*, 3956-3964.
[21] L. Wang, L. Tao, M. Xie, G. Xu, *Catal. Lett.* **1993**, *21*, 35-41.
[22] C. Gueret, M. Daroux, F. Billaud, *Chem. Eng. Sci.* **1997**, *52*, 815-827.
[23] M. Steinberg, *Int. J. Hydrogen Energy* **1999**, *24*, 771-777.
[24] C. Karakaya, S. H. Morejudo, H. Y. Zhu, R. J. Kee, *Ind. Eng. Chem. Res.* **2016**, *55*, 9895-9906.
[25] K. S. Wong, J. W. Thybaut, E. Tangstad, M. W. Stocker, G. B. Marin, *Microporous Mesoporous Mater.* **2012**, *164*, 302-312.
[26] H. Kitagawa, Y. Sendoda, Y. Ono, *J. Catal.* **1986**, 12-18.
[27] V. T. T. Ha, L. V. Tiep, P. Meriaudeau, C. Naccache, *J. Mol. Catal. A: Chem.* **2002**, *181*, 283-290.
[28] Y. Shu, D. Ma, L. Xu, Y. Xu, X. Bao, *Catal. Lett.* **2000**, *70*, 7.
[29] E. V. Matus, I. Z. Ismagilov, O. B. Sukhova, V. I. Zaikovskii, L. T. Tsikoza, Z. R. Ismagilov, J. A. Moulijn, *Ind. Eng. Chem. Res.* **2007**, *46*, 4063-4074.
[30] D. M. Bibby, N. B. Milestone, J. E. Patterson, L. P. Aldridge, *J. Catal.* **1986**, *97*, 493-502.
[31] S. Natesakhawat, N. C. Means, B. H. Howard, M. Smith, V. Abdelsayed, J. P. Baltrus, Y. Cheng, J. W. Lekse, D. Link, B. D. Morreale, *Catal. Sci. Technol.* **2015**, *5*, 5023-5036.
[32] Y.-H. Kim, R. W. I. Borry, E. Iglesia, *Microporous Mesoporous Mater.* **2000**, *35-36*, 15.
[33] R. J. Argauer, G. R. Landolt, *Vol. 3,702,886* (Ed.: U. S. P. Office), United States, **1972**, p. 16.
[34] D. H. Olson, G. T. Kokotallo, S. L. Lawton, W. M. Meier, *J. Phys. Chem.* **1981**, *85*, 2238-2243.
[35] M. E. Leonowicz, J. A. Lawton, S. L. Lawton, M. K. Rubin, *Science* **1994**, *264*, 1910-1913.
[36] A. Corma, C. Corell, J. Perez-Pariente, *Zeolites* **1995**, *15*, 2-8.
[37] D. Ma, Y. Shu, M. Cheng, Y. Xu, X. Bao, *J. Catal.* **2000**, *194*, 105-114.
[38] X. Yin, N. Chu, J. Yang, J. Wang, Z. Li, *Catal. Commun.* **2014**, *43*, 218-222.
[39] H. Liu, S. Yang, J. Hu, F. Shang, Z. Li, C. Xu, J. Guan, Q. Kan, *Fuel Process. Technol.* **2012**, *96*, 195-202.
[40] A. Martinez, E. Peris, *Appl. Catal., A.* **2016**, *515*, 32-44.
[41] M. M. Yung, W. S. Jablonski, K. A. Magrini-Bair, *Energy Fuels* **2009**, *23*, 14.
[42] J. N. Chheda, G. W. Huber, J. A. Dumesic, *Angew. Chem. Int. Ed.* **2007**, *46*, 20.
[43] M. M. Yung, A. K. Starace, C. Mukarakate, A. M. Crow, M. A. Leshnov, K. A. Magrini, *Energy Fuels* **2016**, *30*, 5259-5268.
[44] F. Cheng, V. Dupont, M. V. Twigg, *Appl. Catal., B.* **2017**, *200*, 21-132.
[45] M. Kaewpanha, G. Guan, Y. Ma, X. Hao, Z. Zhang, P. Reubroychareon, K. Kusakabe, A. Abudula, *Int. J. Hydrogen Energy* **2015**, *40*, 9.
[46] J. Li, L. Liu, Y. Liu, Y. Zhu, H. Liu, Y. Kou, J. Zhang, Y. Han, D. Ma, *Energy Environ. Sci.* **2014**, *7*, 393-398.
[47] E. de Smit, F. Cinquini, A. M. Beale, O. V. Safonova, W. van Beek, P. Sautet, B. M. Weckhuysen, *J. Am. Chem. Soc.* **2010**, *132*, 14928-14941.
[48] S. Yun, H. Zhang, H. Pu, J. Chen, A. Hagfeldt, T. Ma, *Adv. Energy Mater.* **2013**, *3*, 1407-1412.
[49] T. Prasomsri, M. Shetty, K. Murugappan, Y. Roman-Leshkov, *Energy Environ. Sci.* **2014**, *7*, 2660-2669.
[50] J. Kim, G. T. Neumann, N. D. McNamara, J. C. Hicks, *J. Mater. Chem.* **2014**, *34*, 14014-14027.
[51] M. G. Montiano, E. Diaz-Faes, C. Barriocanal, R. Alvarez, *Fuel* **2014**, *116*, 175-182.
[52] H. J. Park, S. H. Park, J. M. Sohn, J. Park, J.-K. Jeon, S.-S. Kim, Y.-K. Park, *Bioresour. Technol.* **2010**, *101*, 3.
[53] L. S. Macedo, D. R. Stellwagen, V. T. da Silva, J. H. Bitter, *ChemCatChem* **2015**, *7*, 2816-2823.
[54] S. Li, A. Li, S. Krishnamoorthy, E. Iglesia, *Catal. Lett.* **2001**, *77*, 9.
[55] M. Ding, Y. Yang, B. Wu, Y. Li, T. Wang, L. Ma, *Energy Procedia* **2014**, *61*, 2267-2270.
[56] S. Janbroers, P. A. Crozier, H. W. Zandbergen, P. J. Kooyman, *Appl. Catal., B.* **2011**, *102*, 7.
[57] C.-F. Huo, Y.-W. Li, J. Wang, H. Jiao, *J. Am. Chem. Soc.* **2009**, *131*, 14713-14721.
[58] D. B. Bukur, K. Okabe, M. P. Rosynek, C. Li, D. Wang, K. R. P. M. Rao, G. P. Huffman, *J. Catal.* **1995**, *155*, 353-365.
[59] D.-V. N. Vo, A. A. Adesina, *Appl. Catal., A.* **2011**, *399*, 12.
[60] H. Okamoto, *J. Phase Equilib.* **1992**, *13*, 543-565.
[61] H. L. Yakel, *Int. Mater. Rev.* **1985**, *30*, 17-44.
[62] J. A. Ameise, J. B. Butt, L. H. Schwartz, *J. Phys. Chem.* **1978**, *82*, 6.
[63] Y.-Y. Ji, H.-W. Xiang, J.-L. Yang, Y.-Y. Xu, Y.-W. Li, B. Zhong, *Appl. Catal., A.* **2001**, *214*, 77-86.
[64] Q. Yan, C. Wan, J. Liu, J. Gao, F. Yu, J. Zhang, Z. Cai, *Green Chem.* **2013**, *15*, 10.
[65] K. Sudsakorn, J. G. J. Goodwin, A. A. Adeyiga, *J. Catal.* **2003**, *213*, 204-210.
[66] R. L. Espinoza, A. P. Steynberg, B. Jager, A. C. Vosloo, *Appl. Catal., A.* **1999**, *186*, 13-26.
[67] Y. Ma, G. Guan, C. Shi, A. Zhu, X. Hao, Z. Wang, K. Kusakabe, A. Abdula, *Int. J. Hydrogen Energy* **2014**, *39*, 9.
[68] A. Hanif, T. Xiao, A. P. E. York, J. Sloan, M. L. H. Green, *Chem. Mater.* **2002**, *14*, 7.
[69] T. Zhou, A. Liu, Y. Mo, H. Zhang, *J. Phys. Chem. A.* **2000**, *104*, 4505-4513.

[70] J. Gao, Y. Zhen, J.-M. Jehng, Y. Tang, I. E. Wachs, S. G. Podkolzin, *Science* **2015**, *348*, 5.
[71] H. H. Hwu, J. G. Chen, *Chem. Rev.* **2005**, *105*, 28.
[72] W.-F. Chen, C.-H. Wang, K. Sasaki, N. Marinkovic, W. Xu, J. T. Muckerman, Y. Zhu, R. R. Adzic, *Energy Environ. Sci.* **2013**, *6*, 9.
[73] A. S. Rocha, V. L. T. da Silva, A. A. Leitao, M. H. Herbst, A. C. J. Faro, *Catal. Today* **2004**, *98*, 8.
[74] W. Xu, P. J. Ramirez, D. Stacchiola, J. L. Brito, J. A. Rodriguez, *Catal. Lett.* **2015**, *145*, 9.
[75] C. Karakaya, H. Zhu, R. J. Kee, *Chem. Eng. Sci.* **2015**, *123*, 474-486.
[76] A. J. Medford, A. Vojvodic, F. Studt, F. Abild-Pedersen, J. K. Norskov, *J. Catal.* **2012**, *290*, 10.
[77] M. J. Ledoux, P. Del Gallo, C. Pham-Huu, A. P. E. York, *Catal. Today* **1996**, *27*, 6.
[78] J. S. Lee, M. H. Yeom, K. Y. Park, I.-S. Nam, J. S. Chung, Y. G. Kim, S. H. Moon, *J. Catal.* **1991**, *128*, 126-136.
[79] P. L. Tan, Y. L. Leung, S. Y. Lai, C. T. Au, *Appl. Catal., A.* **2002**, *228*, 115-125.
[80] J. S. Lee, *Catal. Lett.* **1993**, *20*, 97-106.
[81] H. Luo, I. M. Klein, Y. Jiang, H. Zhu, B. Liu, H. I. Kenttamaa, M. M. Abu-Omar, *ACS Sustainable Chem. Eng.* **2016**, *4*, 2316-2322.
[82] J. Kang, R. Han, J. Wang, L. Yang, G. Fan, F. Li, *Chem. Eng. J.* **2015**, *275*, 36-44.
[83] B. Yu, Q. Zhang, L. Hou, S. Wang, M. Song, Y. He, H. Huang, J. Zhou, *Carbon* **2016**, *96*, 904-910.
[84] C. Li, M. Zheng, A. Wang, T. Zhang, *Energy Environ. Sci.* **2012**, *5*, 8.
[85] R. P. W. J. Struis, D. Bachelin, C. Ludwig, A. Wokaun, *J. Phys. Chem. C.* **2009**, *113*, 2443-2451.
[86] W. Vogel, *J. Phys. Chem. C.* **2011**, *115*, 1506-1512.
[87] V. Keller, P. Wehrer, F. Garin, R. Ducros, G. Maire, *J. Catal.* **1995**, *153*, 9-16.
[88] S. Decker, A. Lofberg, J.-M. Bastin, A. Frennet, *Catal. Lett.* **1997**, *44*, 11.
[89] M. G. Alvarez, R. J. Chimentao, D. Tichit, J. B. O. Santos, A. Dafinov, L. B. Modesto-Lopez, J. Rosell-Llompart, E. J. Guell, F. Gispert-Guirado, J. Llorca, F. Medina, *Microporous Mesoporous Mater.* **2016**, *219*, 10.
[90] J. Song, M. Bernien, C.-B. Wu, W. Kuch, *J. Phys. Chem. C.* **2016**, *120*, 1546-1555.
[91] V. Y. Ulianitsky, D. V. Dudina, I. S. Batraev, D. K. Rybin, N. V. Bulina, A. V. Ukhina, B. B. Bokhonov, *Mater. Lett.* **2016**, *181*, 127-131.
[92] J.-S. Choi, G. Bugli, G. Djega-Mariadassou, *J. Catal.* **2000**, *193*, 10.
[93] G. Berhault, A. Mehta, A. C. Pavel, J. Yang, L. Rendon, M. J. Yacaman, L. C. Araiza, A. D. Moller, R. R. Chianelli, *J. Catal.* **2001**, *198*, 11.
[94] S. Jones, P. Meyer, L. Snowden-Swan, A. Padmaperuma, E. Tan, A. Dutta, J. Jacobson, K. Cafferty, National Renewable Energy Laboratory (NREL), Golden, CO., **2013**.
[95] C. H. Bartholomew, *Appl. Catal. A.* **2001**, *212*, 17-60.
[96] P. Forzatti, L. Lietti, *Catal. Today* **1999**, *52*, 165-181.
[97] S. A. Eliason, C. H. Bartholomew, *Appl. Catal., A.* **1999**, *186*, 229-243.
[98] A. Nakhaei Pour, M. R. Housaindokht, *J. Nat. Gas Sci. Eng.* **2013**, *14*, 49-54.
[99] Z. Wang, X. M. Cao, J. Zhu, P. Hu, *J. Catal.* **2014**, *311*, 469-480.
[100] J.-S. Choi, A. H. Zacher, H. Wang, M. V. Olarte, B. L. Armstrong, H. M. Meyer, I. I. Soykal, V. Schwartz, *Energy Fuel* **2016**, *30*, 5016-5026.
[101] D. C. LaMont, A. J. Gilligan, A. R. S. Darujati, A. S. Chellappa, W. J. Thomson, *Appl. Catal., A* **2003**, *255*, 239-253.
[102] S. Takenaka, H. Ogihara, K. Otsuka, *J. Catal.* **2002**, *208*, 54-63.
[103] H.-M. Wang, X.-H. Wang, M.-H. Zhang, X.-Y. Du, W. Li, K.-Y. Tao, *Chem. Mater.* **2007**, *19*, 8.
[104] T. Xiao, H. Wang, J. Da, K. S. Coleman, M. L. H. Green, *J. Catal.* **2002**, *211*, 9.
[105] K. Mai, T. Elder, L. H. Groom, J. J. Spivey, *Catal. Commun.* **2015**, *65*, 76-80.
[106] M. C. Ribeiro, G. Jacobs, B. H. Davis, D. C. Cronauer, A. J. Kropf, C. L. Marshall, *J. Phys. Chem. C.* **2010**, *114*, 7895-7903.
[107] P. Sharma, T. Elder, L. H. Groom, J. J. Spivey, *Top. Catal.* **2014**, *57*, 526-537.
[108] V. Abdelsayed, D. Shekhawat, M. W. Smith, *Fuel* **2015**, *139*, 401-410.
[109] A. Zhang, A. Zhu, B. Chen, S. Zhang, C. Au, C. Shi, *Catal. Commun.* **2011**, *12*, 803-807.
[110] S. Shah, O. G. Marin-Flores, M. G. Norton, S. Ha, *J. Power Sources* **2015**, *294*, 530-536.
[111] N. Ji, T. Zhang, M. Zheng, A. Wang, H. Wang, X. Wang, J. G. Chen, *Angew. Chem.* **2008**, *120*, 4.
[112] R. Ooms, M. Dusselier, J. A. Geboers, B. O. de Beek, R. Verhaeven, E. Gobechiya, J. A. Martens, A. Redl, B. F. Sels, *Green Chem.* **2014**, *16*, 695-707.
[113] M. Koike, D. Li, H. Watanabe, Y. Nakagawa, K. Tomishige, *Appl. Catal., A.* **2015**, *506*, 151-162.

MINIREVIEW

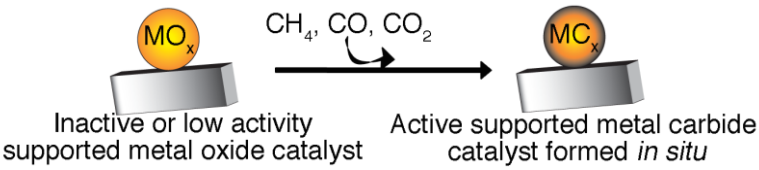

In Situ Carburization: Many catalysts employed in Fischer-Tropsch synthesis, methane dehydroaromatization, and biomass conversion reactions require carburization of the metal before becoming active catalyst species. Often this carburization is performed *in situ* with a carbon containing source gas. This review aims to look at this process across multiple reactions, highlighting influencing factors and recent progress and improvements in the field.

*Megan M. Moyer, Canan Karakaya, Robert J. Kee, Brian G. Trewyn**

Page No. – Page No.

***In Situ* Formation of Metal Carbide Catalysts**